

Energy wave propagation in pristine and bi-crystal graphene

Ying Wang*, Shuai Xu*, Zishun Liu*[†] and Teng Yong Ng[‡]

**International Center for Applied Mechanics
State Key Laboratory for Strength and Vibration of Mechanical Structure
Xi'an Jiaotong University, Xi'an 710049, P. R. China*

*†School of Mechanical and Aerospace Engineering
Nanyang Technological University
50 Nanyang Avenue, Singapore 639798, Singapore
‡zishunliu@mail.xjtu.edu.cn*

Received 4 August 2016
Revised 26 August 2016
Accepted 29 August 2016
Published 22 September 2016

This study investigates the distribution and propagation of potential energy in graphene under tearing loads. Before crack extension, high potential energy accumulates at the crack tip. The distributions of the high potential energy are symmetrical and asymmetrical in pristine graphene and bi-crystal graphene with misorientation angle of 21.79° , respectively. When a C–C bond breaks during the fracture of graphene, numerous energy waves successively arise from the crack tip, i.e., the two atoms linked by the broken bond. These atoms lose one bond constraint and turn into unstable states, and they displace with high accelerations. In pristine graphene, the energy waves present as hexagonal geometries, while the waveforms near the loading areas are compressed to flatter geometries. In bi-crystal graphene, the refractions of potential energy waves are observed when the energy waves propagate to the grain boundary (GB) and interact with it, and the waveforms are changed after the wave crosses the GB. For both pristine graphene and bi-crystal graphene, wrinkles are generated when the crack tip extends to the site sufficiently close to the vertical free boundary, and the wrinkles are always nearly parallel to the horizontal free boundary and move along with the motion of the crack tip.

Keywords: Graphene; grain boundary; tear; energy wave.

1. Introduction

Although early studies since 1947 (Wallace, 1947) focused on graphene's electronic structure, these research efforts on graphene remained in the theoretical realm until graphene was synthesized by exfoliation approach in the laboratory (Geim and Novoselov, 2007). Traditional notion repudiates that two-dimensional material is able to exist independently in reality, but this was discredited by the significant discovery of graphene, which has a single-atom thickness of 0.34 nm. Thus, graphene

[‡]Corresponding author.

also can be regarded as the basic unit of graphite and carbon nanotube. From recent studies on graphene, it has been proven to be the thinnest, strongest, transparent, heat-conducting and electrically conductive material. These impressive properties have attracted significant attention and resulted in graphene being applied in many areas, such as the micro-electro-mechanical systems (MEMS) (Martin-Olmos *et al.*, 2013) and nano-electro-mechanical systems (NEMS) (Lebedeva *et al.*, 2012). Graphene also can be used to construct composite materials by combining with materials such as PMMA or carbon nanotube (Ramanathan *et al.*, 2008; Zhan *et al.*, 2013; Meng *et al.*, 2014). Although pristine graphene has wonderful potential applications, defects cannot be ignored in practical applications. As we know, in the synthesis of graphene, the exfoliation approach is not a mass-production process, and chemical vapor deposition (CVD) has been found to be more feasible to fabricate graphene at a larger scale. However, accompanied with graphene produced by CVD, grain boundary (GB) comprised of the pentagon–heptagon defects acting as a one-dimensional defect which always affects the properties of graphene has been discussed in detail in the study (Kim, 2010; Mattevi *et al.*, 2011). For large flakes of graphene under stretching loads, recent studies show that the strength of polycrystalline graphene is not weakened by the GBs compared with the pristine graphene (Lee *et al.*, 2013; Jung *et al.*, 2015). However, there are many studies which prove that the size and crystal orientation of each grain comprised of bi-crystal or polycrystalline graphene are crucial factors affecting its strength (Yip, 2004; Liu *et al.*, 2011; Wei *et al.*, 2012; Kotakoski and Meyer, 2012; Song *et al.*, 2013). The GBs play the major role on the fracture process when the polycrystalline graphene is subjected to more concentrated loads, such as the nanoindentation load case. The experimental studies by using scanning electron microscope (SEM) show that the failure strengths of polycrystalline graphene are reduced to less than half of the strength of pristine graphene under the concentrated loading case (Suk *et al.*, 2015). From molecular dynamics (MD) simulation, the rupture processes during the nanoindentation test are clearly presented, and the loading position of the point load also has a significant effect on the fracture pattern, such as whether the site is located on the junction of GBs or not (Sha *et al.*, 2014; Han *et al.*, 2016).

For the thin film materials such as extensible connective tissues and graphene, tearing behavior can be prevalent (Purslow, 1983), and this behavior is also a convenient and efficient process to tailor a large flake material into the proper dimensions or to measure the fracture toughness of the materials. So, there is engineering significance to study tearing a large piece of graphene into small pieces. For tearing graphene from the matrix, the results of the first-principles ReaxFF MD and experimental studies show that the shape of graphene nanoribbons are tapered and the tapered angles are determined by the adhesive energy between graphene and matrix (Sen *et al.*, 2010). For suspended graphene under the tearing load, through tight-binding MD simulation, researchers have found that the rupture of C–C bonds are always along the zigzag direction regardless of the direction of initial crack (Kawai

et al., 2009). However, the first-principles ReaxFF MD simulations show contrary results where the armchair direction is the favored path for the crack propagation in the suspended graphene under tearing force (Huang *et al.*, 2012). Accordingly, previous studies show that the preferred direction of crack propagation for tearing the suspended graphene is relatively fixed to the zigzag or armchair directions, which is different from the tensile case in which the fracture path is dependent on the initial crack direction (Kim *et al.*, 2011).

Having sufficient energy is crucial for dynamic crack propagation in materials, and the transmission velocity of the energy directly influences the fracture process. Many studies have illustrated that the velocity of energy propagation is limited by the wave velocity in materials (e.g., longitudinal or shear wave etc.), and this restricts the crack propagation velocity (Jia *et al.*, 2012; Abraham and Gao, 2000; Koizumi *et al.*, 2007). Therefore, to understand the dynamic fracture of graphene under the tearing force, it is imperative to determine the mode of energy transmission. There are various waves in materials caused by different factors (Islam *et al.*, 2014; Kamali *et al.*, 2016; Kuzmin, 2015). Earlier studies reveal that water-like wave characterized by the out-plane displacement forms when graphene is struck by the point load, and also report how the heat wave propagates in pristine graphene (He *et al.*, 2011; Wang and Lee, 2012; Arash *et al.*, 2012). Compared with the pristine graphene, the effect of Stone–Wales (SW) defect or vacancies on the ripples propagation in defective graphene is significant and limited near the point defect (Dong *et al.*, 2014).

In this paper, we focus on the suspended graphene under the tearing force. The MD simulations on the energy wave propagation in graphene are carried out by using large-scale atomic/molecular massively parallel simulator (LAMMPS). The results show that high potential energy in pristine graphene is almost symmetrically distributed along the crack track, and the regular hexagon waveforms are observed for the part of energy wave far away from the loading areas, but the waveforms near the loading area are flattened. For the bi-crystal graphene, the GB has significant influence on the distribution of the energy, and the atoms with high potential energy no longer scatter symmetrically along the crack length. It is also noted that the waveforms of the energy waves in bi-crystal graphene are changed by the GB, and obvious refraction is observed when the energy wave propagates to the GB. Furthermore, when the crack tip is closed to the vertical free boundary, there are some wrinkles observed, approximately parallel to another horizontal free boundary.

2. Models and Methods

Figure 1 describes the schematics of simulated graphene model with the size about $50\text{ nm} \times 50\text{ nm}$. In this paper, we establish two typical models, including the pristine graphene and the bi-crystal graphene with misorientation angle of 21.79° (Liu *et al.*, 2011). For the bi-crystal graphene, the GB is distributed with pentagon–heptagon

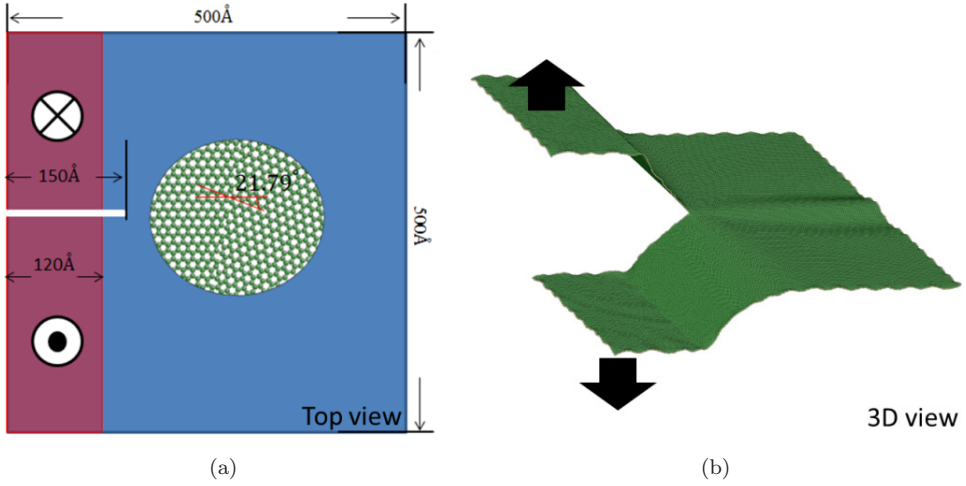


Fig. 1. (Color online) (a) The schematic for the tearing models of bi-crystal graphene for misorientation angle of 21.79° . The atomic structure embedded reveals the lattice on both sides of the GB. The arrowhead and tail of the arrows present the direction of the applied tearing force, and the places covered by the red color are moved along the arrowhead. (b) The atomic snapshot shows the geometry of graphene in the tearing process.

defects, and the lattice structure of the crystals forming the bi-crystal graphene is symmetric with respect to the GB, as shown in Fig. 1(a). The initial crack is set along the zigzag direction on the edge of the models. To avoid “self-healing” of some atoms during relaxing process due to the small width, the crack is set at two or three atom width, while its length is about 15 nm (> 10 nm was reported as a proper length value in reference (Yin *et al.*, 2015)).

Herein, the open-source software LAMMPS is used to perform the MD simulation and the simulation results are analyzed with the aid of atomistic configuration viewer (AtomEye). The adaptive intermolecular reactive empirical bond order (AIREBO) is adopted in our simulations, which is a popular potential function to describe the atomic interaction of carbon atoms or hydrogen atoms. This potential has also been used in many previous studies (He *et al.*, 2014). In our MD simulation, we make use of the canonical ensemble (NVT) to keep the system homothermal state at around 1 K. To apply tearing loads, the loading locations indicated by red color are moved at $1 \text{ \AA}/\text{ps}$ in two opposite directions, the arrows shown in Fig. 1(b) represent the loading directions.

3. Results

3.1. *The propagation and distribution of high potential energy in pristine graphene*

Energy distribution dictates the mechanical behavior of graphene, and here we investigate the energy propagation in graphene to understand the mechanical properties

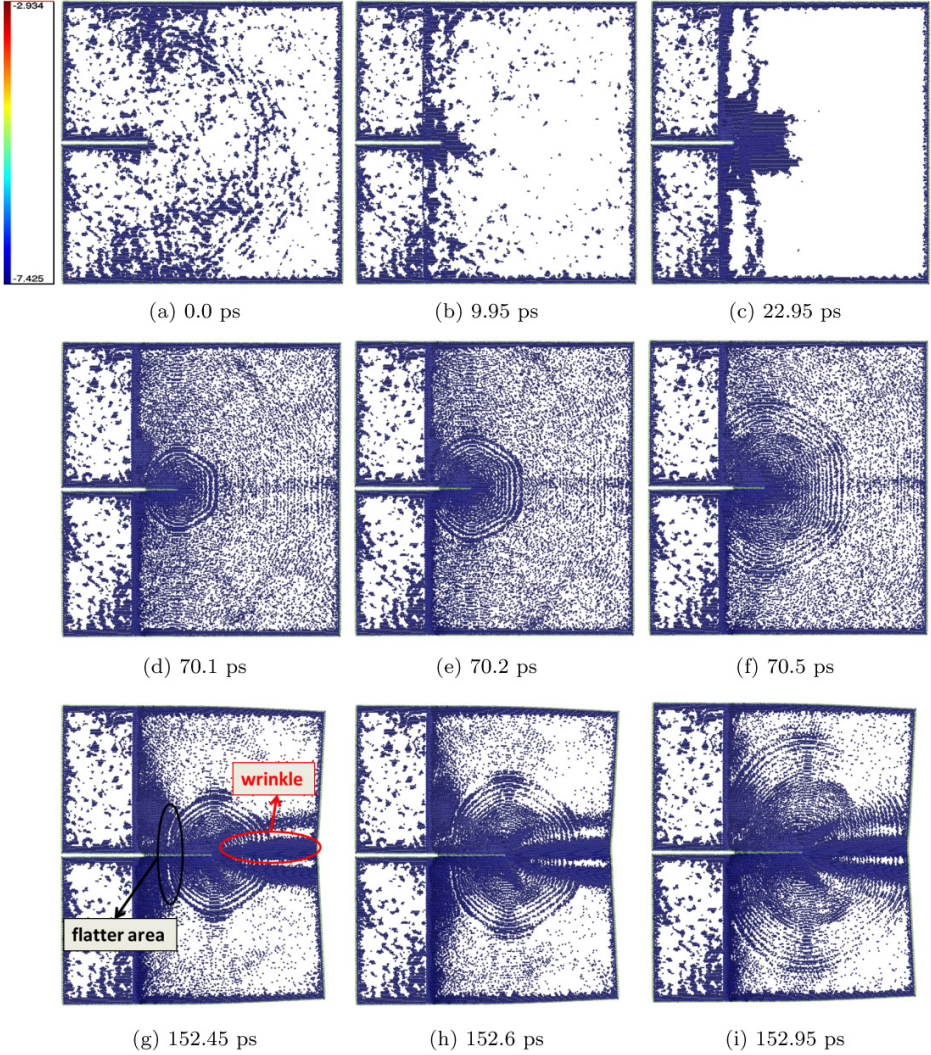


Fig. 2. (Color online) Snapshots at different times with atoms in pristine graphene visualizing only the high potential energy. (a)–(c) The snapshots of the symmetric energy distribution around the crack tip in pristine graphene before the crack grows. The figures are obtained at three different times. (d)–(f) and (g)–(i), the snapshots of the propagating energy wave just after two C–C bonds are broken, respectively.

of graphene through MD simulation. Figures 2(a)–2(i) show snapshots of atoms capturing the high potential energy ranges from -7.425 eV to -2.934 eV, in which the atoms with lower potential energy are not visualized, and the kinetic energy of atoms is ignored in the snapshots. Before the crack in graphene extends under the tearing force, it shows that the high energy gradually accumulates around the crack tip, and distributes almost symmetrically with respect to the extension line of the

initial crack, as shown in Figs. 2(a)–2(c). When the energy in the graphene is high enough to drive the crack to extend, the C–C bonds break continuously, and the crack path always forms the zigzag edges. The rupture of the C–C bond transforms the carbon atom from the sp^2 hybridization to sp hybridization. Meanwhile, the stable state of the carbon atoms is lost when the C–C bond is just broken. Thus, before reaching another stable state, the unstable carbon atoms move with accelerations produced by the lost constraint, which generate a series of potential energy waves from the crack tip. Then the irregular motion of two atoms would make the surrounding atoms move, and the motion is transmitted through the involvement of more atoms in the subsequent motion, which is exhibited as the propagation of potential energy, as shown in Figs. 2(d)–2(i). Therefore, the result implies that a series of potential energy waves are produced from the crack tip whenever a C–C bond is destroyed and the waves are spread around during the fracture process under the tearing force.

As shown in Figs. 2(d)–2(f), a C–C bond breaks during the tearing process, meanwhile, the potential energy waves are generated and transfer in graphene. The results show that the geometry of the waves far away from the loading areas are approximately regular hexagonal. However, the wave surfaces near the loading area are squeezed into approximately elliptical shape. Once the atoms linked by the broken C–C bond tend toward a stable state, the waves are not newly created anymore, and the existing energy waves gradually dissipate and disappear during the propagating process until the next C–C breaks.

Figures 2(g)–2(i) display the potential energy wave propagation in graphene when another C–C bond breaks. During this process, we find that wrinkles appear at the front of the crack tip, and high energy accumulates there. The wrinkles are also gradually formed during the fracture process under the tearing force, and it becomes relatively obvious and can be observed at about 84.15 ps. The potential energy distributes symmetrically along the crack path. In addition, there exists an approximate high energy triangle in the zone between the loading area and the crack tip, as that region is tightly stretched to break the C–C bond during the fracture process. It can also be seen that the waveforms of the potential energy wave far away from the loading area are still relatively hexagonal, but the shape is not as regular as that in pristine graphene. Near the loading area, the waves are flatter than other areas, which implies that the propagation of potential energy wave is hindered by the loading areas. However, the waveforms near the free boundary do not change to be flatter, thus the boundary never stops the propagation of the potential energy waves.

3.2. The interaction between the GB and the potential energy wave in bi-crystal graphene

As a benchmark comparison with pristine graphene, Figs. 3(a)–3(i) show that the potential energy accumulates in the bi-crystal graphene with a misorientation angle

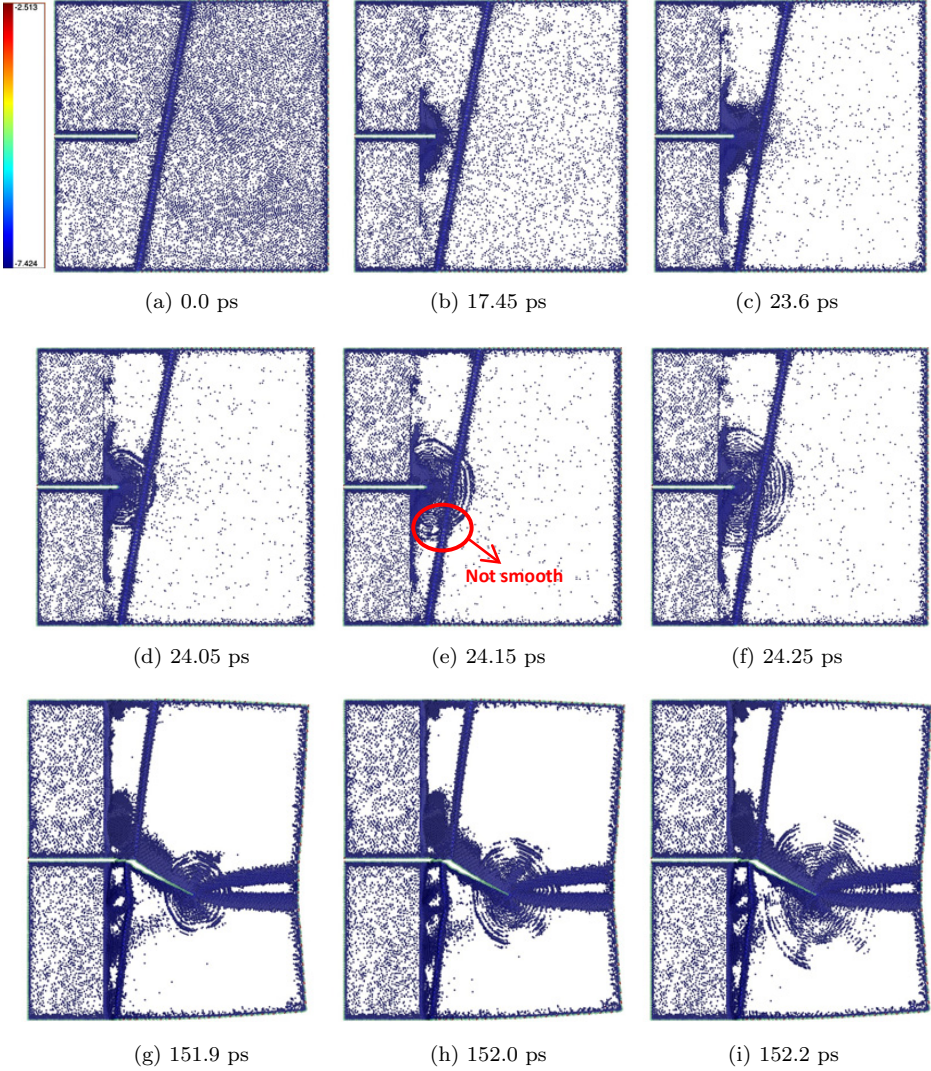


Fig. 3. (Color online) Snapshots at different times with atoms in bi-crystal graphene with the misorientation of 21.79° visualizing only the high potential energy. (a)–(c): The snapshots of the energy distribution around the crack tip in bi-crystal graphene before the crack grows. (d)–(f) and (g)–(i), the snapshots of the propagating energy wave caused by the breakage of two different C–C bonds, respectively.

of 21.79° under the tearing force. From Figs. 3(a)–3(c), it can be found that almost all the high potential energy accumulates in the area around the crack tip before the first C–C bond breaks. However, the distribution of the energy is asymmetric with respect to the extension line of the initial crack, when the high energy increases and interacts with the GB, as shown in Fig. 3(c). The asymmetric energy distribution indicates that the GB has a significant effect on the energy accumulation.

When the crack begins extending along the zigzag direction and does not cross the GB, the GB could also influence the propagation path of the energy wave as shown in Figs. 3(d)–3(f). Different from the pristine graphene, the waveforms of the energy waves are no longer regular hexagonal, and it can be observed that the junctions of the waveforms on the two sides of the GB are not smooth, thus implying that the propagating orientation of the wave has changed after it crosses the GB. It also indicates that the potential energy waves refract when the waves directly cross the GB which are regarded as the interface between two single-crystal graphene with different lattice directions. After crossing the GB, the potential energy wave continues propagating forward in graphene.

Under the tearing force, the crack crosses the GB but does not follow it, which is consistent with the results of Kwanpyo Kim for the stretching case (Kim *et al.*, 2011), and the crack track is always following zigzag direction in this study. It can be found that the energies around the crack are especially asymmetric to the crack path after the crack extends across the GB. Furthermore, similar to the pristine graphene, the wrinkles, which are manifested by the high energy, gradually form at the front of the crack tip in bi-crystal graphene under the tearing force. The wrinkles become obvious at about 110.8 ps, which are similar to the pristine graphene. Thus, it can be concluded that the wrinkles are formed because the crack tip approaches the free boundary, which indicates that the free boundary is an important factor for the wrinkles. From Figs. 3(g)–3(i), it can be observed that these wrinkles are almost always parallel to the horizontal free boundary rather than the crack path, and they will move along with the extending crack tip.

4. Concluding Remarks

In this study, we performed MD simulations to investigate the properties of the energy wave in pristine and bi-crystal graphene under tearing load, and examined the propagation mechanism of the energy wave during the failure process. We explore the energy in the pristine and bi-crystal graphene by hiding the atoms which have lower potential energy and only visualizing the atoms with higher potential energy. The results show that the high energy distributes symmetrically around the extension line of the crack in pristine graphene, while it is asymmetrical in the bi-crystal graphene, especially after the crack extended the GB. Once a C–C bond breaks, a series of energy waves generate and propagate all around. The origin of the energy wave is the unstable atoms which lose a constraint. In the failure process, the loading area will restrict the propagation of the energy wave in both pristine and bi-crystal graphene. The GB acting as the interface of two single-crystal graphene with different lattice orientations interacts with the energy wave in the bi-crystal graphene. Furthermore, wrinkles which are nearly parallel to the horizontal free boundary form at front of the crack tip and move with the extending of the crack.

Acknowledgments

WY, XS and LZS are grateful for the support from the National Natural Science Foundation of China through Grant Nos. 11372236, 11572236 and 11321062.

References

- Abraham, F. F. and Gao, H. [2000] “How fast can cracks propagate?,” *Phys. Rev. Lett.* **84**(14), 3113.
- Arash, B., Wang, Q. and Liew, K. M. [2012] “Wave propagation in graphene sheets with nonlocal elastic theory via finite element formulation,” *Comput. Methods Appl. Mech. Eng.* **223**, 1–9.
- Dong, Y., He, Y., Wang, Y. and Li, H. [2014] “A theoretical study of ripple propagation in defective graphene,” *Carbon* **68**, 742–747.
- Geim, A. K. and Novoselov, K. S. [2007] “The rise of graphene,” *Nat. Mater.* **6**(3), 183–191.
- Han, J., Ryu, S. and Sohn, D. [2016] “A feasibility study on the fracture strength measurement of polycrystalline graphene using nanoindentation with a cylindrical indenter,” *Carbon* **107**, 310–318.
- He, L. C., Guo, S. S., Lei, J. C., Sha, Z. D. and Liu, Z. S. [2014] “The effect of Stone–Thrower–Wales defects on mechanical properties of graphene sheets—A molecular dynamics study,” *Carbon* **75**, 124–132.
- He, Y. Z., Li, H., Si, P. C., Li, Y. F., Yu, H. Q., Zhang, X. Q., Ding, F., Liew, K. M. and Liu, X. F. [2011] “Dynamic ripples in single layer graphene,” *Appl. Phys. Lett.* **98**(6), 063101.
- Huang, X., Yang, H., van Duin, A. C., Hsia, K. J. and Zhang, S. [2012] “Chemomechanics control of tearing paths in graphene,” *Phys. Rev. B* **85**(19), 195453.
- Islam, Z. M., Jia, P. and Lim, C. W. [2014] “Torsional wave propagation and vibration of circular nanostructures based on nonlocal elasticity theory,” *Int. J. Appl. Mech.* **6**(02), 1450011.
- Jia, Y. J., Zhu, W. P., Li, T. and Liu, B. [2012] “Study on the mechanisms and quantitative law of mode I supersonic crack propagation,” *J. Mech. Phys. Solids* **60**(8), 1447–1461.
- Jung, G., Qin, Z. and Buehler, M. J. [2015] “Molecular mechanics of polycrystalline graphene with enhanced fracture toughness,” *Extreme Mech. Lett.* **2**, 52–59.
- Kamali, R., Mousavi, S. M. and Khojasteh, D. [2016] “Three-dimensional passive and active control methods of shock wave train physics in a duct,” *Int. J. Appl. Mech.* **08**, 1650047.
- Kawai, T., Okada, S., Miyamoto, Y. and Hiura, H. [2009] “Self-redirection of tearing edges in graphene: Tight-binding molecular dynamics simulations,” *Phys. Rev. B* **80**(3), 033401.
- Kim, P. [2010] “Graphene: Across the border,” *Nat. Mater.* **9**(10), 792–793.
- Kim, K., Artyukhov, V. I., Regan, W., Liu, Y., Crommie, M., Yakobson, B. I. and Zettl, A. [2011] “Ripping graphene: preferred directions,” *Nano Lett.* **12**(1), 293–297.
- Koizumi, H., Kirchner, H. and Suzuki, T. [2007] “Supersonic crack motion in a harmonic lattice,” *Philos. Mag. Lett.* **87**(8), 589–593.
- Kotakoski, J. and Meyer, J. C. [2012] “Mechanical properties of polycrystalline graphene based on a realistic atomistic model,” *Phys. Rev. B* **85**(19), 195447.
- Kuzmin, A. [2015] “Shock wave instability in a channel with an expansion corner,” *Int. J. Appl. Mech.* **7**(02), 1550019.

- Lebedeva, I. V., Knizhnik, A. A., Popov, A. M., Lozovik, Y. E. and Potapkin, B. V. [2012] “Modeling of graphene-based NEMS,” *Physica E* **44**(6), 949–954.
- Lee, G. H., Cooper, R. C., An, S. J., Lee, S., van der Zande, A., Petrone, N., Hammerberg, A. G., Lee, C., Crawford, B. and Oliver, W. [2013] “High-strength chemical vapor-deposited graphene and grain boundaries,” *Science* **340**(6136), 1073–1076.
- Liu, T. H., Gajewski, G., Pao, C. W. and Chang, C. C. [2011] “Structure, energy, and structural transformations of graphene grain boundaries from atomistic simulations,” *Carbon* **49**(7), 2306–2317.
- Martin-Olmos, C., Rasool, H. I., Weiller, B. H. and Gimzewski, J. K. [2013] “Graphene MEMS: AFM probe performance improvement,” *ACS Nano* **7**(5), 4164–4170.
- Mattevi, C., Kim, H. and Chhowalla, M. [2011] “A review of chemical vapor deposition of graphene on copper,” *J. Mater. Chem.* **21**(10), 3324–3334.
- Meng, X. H., Li, M., Xing, Y. L. and Bai, Z. Y. [2014] “A mechanical model for self-assembled graphene around nanotube,” *Int. J. Appl. Mech.* **6**(04), 1450036.
- Purslow, P. P. [1983] “Measurement of the fracture toughness of extensible connective tissues,” *J. Mater. Sci.* **18**(12), 3591–3598.
- Ramanathan, T., Abdala, A. A., Stankovich, S., Dikin, D. A., Herrera-Alonso, M., Piner, R. D., Adamson, D. H., Schniepp, H. C., Chen, X. and Ruoff, R. S. [2008] “Functionalized graphene sheets for polymer nanocomposites,” *Nat. Nanotechnol.* **3**(6), 327–331.
- Sen, D., Novoselov, K. S., Reis, P. M. and Buehler, M. J. [2010] “Tearing graphene sheets from adhesive substrates produces tapered nanoribbons,” *Small* **6**(10), 1108–1116.
- Sha, Z. D., Wan, Q., Pei, Q. X., Quek, S. S., Liu, Z. S., Zhang, Y. W. and Shenoy, V. B. [2014] “On the failure load and mechanism of polycrystalline graphene by nanoindentation,” *Sci. Rep.* **4**, 7437.
- Song, Z. G., Artyukhov, V. I., Yakobson, B. I. and Xu, Z. P. [2013] “Pseudo Hall–Petch strength reduction in polycrystalline graphene,” *Nano Lett.* **13**(4), 1829–1833.
- Suk, J. W., Mancevski, V., Hao, Y., Liechti, K. M. and Ruoff, R. S. [2015] “Fracture of polycrystalline graphene membranes by in situ nanoindentation in a scanning electron microscope,” *Phys. Status Solidi RRL* **9**(10), 564–569.
- Wallace, P. R. [1947] “The band theory of graphite,” *Phys. Rev.* **71**(9), 622.
- Wang, X. Q. and Lee, J. D. [2012] “Heat wave driven by nanoscale mechanical impact between C 60 and graphene,” *J. Nanomech. Micromech.* **2**(2), 23–27.
- Wei, Y. J., Wu, J. T., Yin, H. Q., Shi, X. H., Yang, R. G. and Dresselhaus, M. [2012] “The nature of strength enhancement and weakening by pentagon–heptagon defects in graphene,” *Nat. Mater.* **11**(9), 759–763.
- Yin, H. Q., Qi, H. J., Fan, F. F., Zhu, T., Wang, B. L. and Wei, Y. J. [2015] “Griffith criterion for brittle fracture in graphene,” *Nano Lett.* **15**(3), 1918–1924.
- Yip, S. [2004] “Nanocrystalline metals: mapping plasticity,” *Nat. Mater.* **3**(1), 11–12.
- Zhan, H. F., Xia, K. and Gu, Y. T. [2013] “Tensile properties of graphene-nanotube hybrid structures: a molecular dynamics study,” *Int. J. Comput. Mater. Sci. Struct. Eng.* **2**(03n04), 1350020.